CONCEPTUAL DESIGN OF A HARD LANDING INDICATION SYSTEM USING A FLIGHT PARAMETER SENSOR SIMULATION MODEL

P. Sartor*, R.K. Schmidt, W. Becker*, K. Worden*, D.A. Bond** , W.J. Staszewski***
***University of Sheffield, **Messier-Dowty**

Keywords: *landing gear, hard landing, Bayesian sensitivity study*

Abstract

A Flight Parameter Sensor Simulation (FPSS) model has been developed to assess the conservatism of the landing gear loads calculated using a hard landing analysis process. Conservatism exists due to factors of safety that are added to the hard landing analysis process to account for uncertainty in the measurement of certain flight parameters. The FPSS model consists of: (1) an aircraft and landing gear dynamic model to determine the 'actual' landing gear loads during a hard landing; (2) an aircraft sensor and data acquisition model to represent the aircraft sensors and flight data recorder (FDR) systems to investigate the effect of signal processing on the flight parameters; (3) an automated hard landing analysis process, representative of that used by airframe and equipment manufacturers, to determine the 'simulated' landing gear loads. Using a technique of Bayesian sensitivity analysis, a number of flight parameters are varied in the FPSS model to gain an understanding of the sensitivity of the difference between 'actual' and 'simulated' loads (measured as Mean-Square Error (MSE)) to the individual flight parameters in symmetric, two-point landings. This study shows that the tyre-runway friction coefficient and aircraft vertical descent velocity (V_z) contributed the most to the spin-up and spring-back drag axle response load MSE and bending moment MSE. It was also found that aircraft vertical descent velocity, mass, centre of gravity position and tyre type had significant influences on the maximum vertical reaction vertical axle response load MSE. Due to the modelling technique, it was also found that vertical acceleration was as significant as V_z in reducing the MSE. While ground speed and aircraft pitch did not change considerably from the 'actual' to the 'simulated' landings, their interactions with tyre-runway friction coefficient and aircraft vertical descent velocity contributed to the MSE in all cases. Of equal importance, it was also shown that within the range studied, shock absorber servicing state and tyre pressure do not contribute significantly to the MSE and learning the true value of these flight parameters would not reduce the MSE.

1 Introduction

A static structural overload occurs when landing gear exceeds its material yield point in any location. A common aircraft operational occurrence which may result in a landing gear overload is a hard landing. A hard landing is defined by the regulatory authorities in EASA Certification Specification (CS) 25 and Federal Aviation Regulations (FAR) 25 as a landing with a limit vertical descent velocity exceeding 10 ft/s [1, 2]. However, the effect of the vertical descent velocity must be combined with other critical enveloping flight parameters, including: aircraft gross weight, aircraft centre of gravity location, aircraft orientation (pitch, roll, yaw), rates of motion (pitch rate, roll rate, yaw rate), ground speed, vertical descent velocity, longitudinal, lat-

eral and vertical acceleration, shock absorber servicing state and the tyre-runway friction coefficient, to accurately assess the loads in the landing gear.

If the flight crew suspect that there has been a hard landing, the following analysis process is performed: (i) the flight crew makes an occurrence declaration; (ii) visual and Non-Destructive Testing (NDT) inspections are performed on the landing gear by the operator's maintenance crew to assess for damage to the landing gear and airframe structure; (iii) aircraft flight parameter data, such as aircraft acceleration, ground speed and aircraft orientation (pitch, roll), are downloaded from the Flight Data Recorder (FDR) and reported to the aircraft and landing gear manufacturers, who then calculate the loads during the occurrence at spin-up, spring-back and maximum vertical reaction. Only after the data has been analyzed can it be determined if there has been an overload.

A degree of conservatism exists in the current hard landing analysis process to ensure safety of aircraft operation. This conservatism evolves from factors of safety or conservative assumptions included within the analysis process to account for: (i) uncertainty in measured aircraft flight parameters and (ii) unavailable aircraft flight parameters. For example, vertical acceleration is typically sampled at 8 Hz. A landing however, takes less than 125 ms. Thus, a possibility exists that the peak vertical acceleration recorded on the FDR is less than the actual maximum value. To date, the effect of such assumptions on the degree of conservatism in a hard landing analysis process has not been quantified [3].

A Flight Parameter Sensor Simulation (FPSS) model has been developed to assess the conservatism in a hard landing analysis process [4]. Using a technique of Bayesian sensitivity analysis, a number of flight parameters are varied in the FPSS model to gain an understanding of how the model responds to variations in the inputs, to identify the most influential input parameters and to identify which input parameters have little or no effect on the conservatism [5]. In this technique, an emulator of the model is created by fitting a Gaussian process to the response surface using data from multiple runs of the model as dictated by a Design-of-Experiments (DOE) so that the output of the model can be predicted for any point in the input space without having to run the simulation. Each input parameter is represented as a probability distribution and sensitivity analysis data is inferred at a reduced computational cost and with little loss of accuracy. Computational savings can be up to two orders of magnitude compared to using a Monte Carlo method [6, 7]. Accuracy of the emulator model is dependent on the model and the number of model runs, and can be quantified through cross-validation with the model runs.

This paper first describes the loads of interest when determining the serviceability of the Main Landing Gear (MLG) structure. The FPSS model is then explained. The theoretical background of the Bayesian sensitivity analysis is then presented, including a discussion on Gaussian processes which are used to develop the emulator, and the main effects and sensitivity indices inferred from the resulting distribution-over-functions. Finally, the results of the sensitivity analysis for symmetric landings using the FPSS model are shown.

2 Landing Gear Loads

Figure 1 shows a typical telescopic port MLG structure and Figure 2 illustrates the landing dynamics of the MLG in a two-point, symmetric landing. On approach, the landing gear wheels are not spinning. However on contact with the runway, the landing gear wheels spin-up to the ground speed of the aircraft under the influence of the ground reaction and the tyre-runway friction. The resulting drag force deforms the landing gear aft and stores energy in the structure. When the tyre velocity reaches the aircraft forward speed, the frictional force between the tyre and the ground reduces and the release of the strain energy stored in the rearward deformation produces a spring-back. The landing gear oscillates until the structural damping reduces

the stored energy to zero [8]. Also during this time, there is an increasing vertical ground-to-tyre load, which is a function of the gas spring, oil damping (related to the square of the vertical descent velocity) and bearing friction. The shock absorber continues to close until all the vertical energy has been absorbed and then it partially recoils [9]. The shock absorber travel (SAT), in conjunction with the landing loads, creates a bending moment on the landing gear structure which is computed at the lower bearing.

In order to calculate the internal landing gear loads and to assess the serviceability of the landing gear structure after a hard landing, the axle response loads are required. The ground-to-tyre loads, discussed previously, act as the forcing function and with the mass and flexibility characteristics of the landing gear, produce the dynamic response loads at the landing gear axle. The difference between the ground-to-tyre loads and the axle dynamic response loads is due to the inertia forces of the landing gear mass between the ground and the landing gear axle during the impact [10]. The points of interest for the symmetric landing analysis are the drag axle response load and bending moment at the lower bearing at spin-up and spring-back, and the vertical axle response load at maximum vertical reaction [11].

3 Overview of the Flight Parameter Sensor Simulation Model

The FPSS model, shown in Figure 3, consists of: (1) an aircraft and landing gear dynamic model, (2) an aircraft sensor and data acquisition Simulink model to represent the aircraft FDR and (3) an automated hard landing analysis process. Various hard landing cases, represented as (C_1, C_2, C_3,..., C_m), were modelled using a representative aircraft and landing gear dynamic model. For each of the landing cases, it was possible to define flight parameters such as: aircraft gross weight, aircraft centre of gravity location, aircraft orientation (pitch, roll, yaw), ground speed, vertical descent velocity, lateral velocity, MLG shock absorber servicing state, tyre type, tyre pressure and the tyre-runway friction coefficient. These

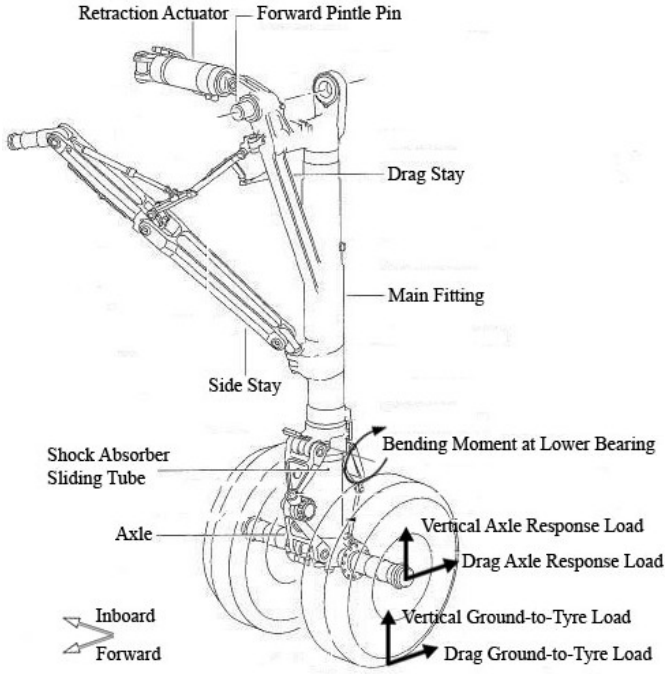

Fig. 1 Typical Port Main Landing Gear Structure

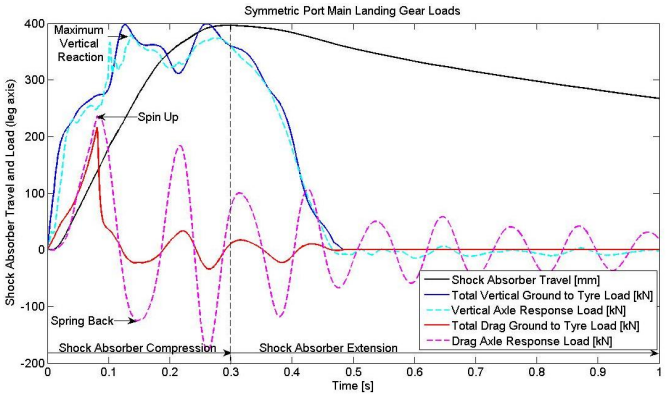

Fig. 2 Example of Occurrence Port Main Landing Gear Landing Dynamics

landing cases provide simulation of the 'actual' flight parameters during the simulation, as well as landing gear dynamic response loads at the axle at spin-up, spring-back and maximum vertical reaction.

The aircraft sensor and data acquisition model (SC_1) represents the aircraft sensors and FDR systems. Aircraft flight parameters such as vertical, longitudinal and lateral accelerations, pitch and roll angle and ground speed are used in the typical hard landing analysis process. A typical aircraft navigation system and indicat-

ing/recording system was modelled in Simulink to investigate the effect of signal processing (sampling rate, filtering, analog to digital conversion, transfer/receive delays) on the aircraft flight parameters.

Finally, with the flight parameter data from the FDR, a hard landing analysis process was modelled and the conservative assumptions typically made were applied. These assumptions include: aircraft mass, inertia and centre of gravity location as close as possible to the occurrence case, assumed tyre type, correctly serviced shock absorber and assumed tire-runway friction coefficient. The peak aircraft vertical acceleration data from the FDR, as well as the other FDR parameters at the peak vertical acceleration, are used to model the symmetric landing gear dynamic axle response loads. Based on the initial conditions provided by the FDR (ground speed, pitch, roll), the aircraft vertical descent velocity was iterated until the aircraft vertical acceleration output from the hard landing analysis process model matched the peak vertical acceleration from the FDR. From the landing gear dynamic axle response loads calculated based on those conditions, it was possible to estimate the difference between the 'actual' and the 'simulated' landing gear loads using a normalized Mean-Square Error (MSE) method:

$$Mean\text{-}Square\ Error_i = \frac{(F_{actual_i} - F_{simulated_i})^2}{\sigma^2_{F_{actual}}} \times 100 \quad (1)$$

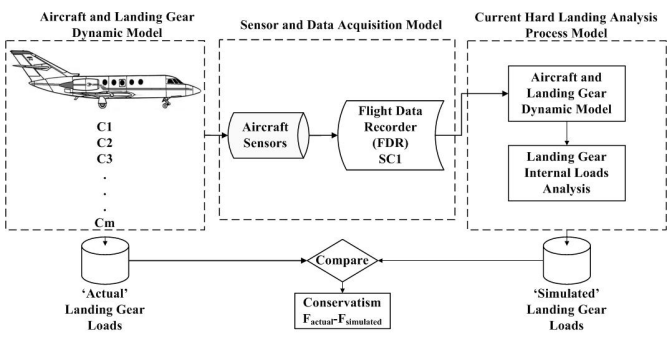

Fig. 3 Flight Parameter Sensor Simulation Model

4 Bayesian Sensitivity Analysis

4.1 Gaussian Processes

Any computer model, such as the FPSS model, can be considered a function of its inputs: $f(\boldsymbol{x})$. Although this function is deterministic and governed by known mathematical functions, it is often complex and may actually be encoded by a large numerical model which has no closed-form expression for its outputs as a function of its inputs. Therefore, $f(\boldsymbol{x})$ could be considered an unknown function, since the output is unknown for a given set of inputs until the model has actually been run. If however, the function (model) is sampled at a number of carefully chosen input points, it is possible to fit a response surface which can predict the output of the model for any point in the input space without having to run the model. For models that are computationally expensive (they require several minutes, hours or days to run), creating an emulator (a model of a model) is a useful approach for sensitivity analysis which requires generally multiple runs of the model under investigation. [6]

A particular probabilistic approach for developing an emulator is the use of Gaussian process regression [12, 13, 14]. Gaussian processes are an extension of a multivariate Gaussian probability distribution. Most forms of regression return a crisp value $f(\boldsymbol{x})$ for any given $\boldsymbol{x}$; however a Gaussian process returns a Gaussian probability distribution. Therefore, for a function, the Gaussian process can be considered a Gaussian probability distribution, where the mean and covariance are specified at any point (or variable) by a mean function and covariance function, respectively.

Gaussian processes adhere to the Bayesian paradigm, such that a number of prior assumptions are made about the function being modelled, and then training data (samples from the model) are used to update and evaluate a posterior distribution over functions. It is assumed that the model is a smooth function so that if the value of $f(\boldsymbol{x})$ is known, the value at $f(\boldsymbol{x}')$ for $\boldsymbol{x}$ close to $\boldsymbol{x}'$ will be highly correlated. This assumption allows information to be gained on the response

surface at reduced computational cost.

For any set of n input parameters $\{x_1,\ldots, x_n\}$, each of dimension d, the prior beliefs about the corresponding outputs can be represented by a multivariate normal distribution, the mean of which is a least-squares regression fit through the training data:

$$E\{f(x)|\beta\} = \boldsymbol{h}(\boldsymbol{x})^T\beta \tag{2}$$

where $\boldsymbol{h}(\boldsymbol{x})^T$ is a specified regression function of $\boldsymbol{x}$, and β is the corresponding vector of coefficients. Here, $\boldsymbol{h}(\boldsymbol{x})^T$ is chosen to be $(1,\boldsymbol{x}^T)$, which represents linear regression. The covariance (cov) between output points is:

$$cov\{f(\boldsymbol{x}),f(\boldsymbol{x}')|\sigma^2,B\} = \sigma^2 c(\boldsymbol{x},\boldsymbol{x}') \tag{3}$$

such that

$$c(\boldsymbol{x},\boldsymbol{x}') = \exp\{-(\boldsymbol{x}-\boldsymbol{x}')^T B(\boldsymbol{x}-\boldsymbol{x}')\} \tag{4}$$

where σ^2 is a scaling factor and B is a diagonal matrix of length-scales, which represent the roughness of the output with respect to the individual input parameters.

The posterior distribution is then found by conditioning the prior distribution on the training data $\boldsymbol{y}$ (the output vector corresponding to the input set), and integrating out the hyperparameters σ^2 and β. This results in a Student's t-process, conditional on B and the training data:

$$[f(\boldsymbol{x})|B,\boldsymbol{y}] \sim t_{n-q}\{m^*(\boldsymbol{x}),\hat{\sigma}^2 c^*(\boldsymbol{x},\boldsymbol{x}')\} \tag{5}$$

where m^* and $c^*(\boldsymbol{x},\boldsymbol{x}')$ are the posterior mean and posterior covariance function respectively and B, $\hat{\beta}$, $\hat{\sigma}^2$ are the hyperparameters of the posterior distribution, the definitions of which can be found in [6]. The quality of the emulator is dependent on the number and distribution of training data points in the input space, and the values of the hyperparameters.

4.2 Inference for Sensitivity Analysis

If the input vector, $\boldsymbol{x}$, is uncertain, $\boldsymbol{X}$, the "true input configuration" is considered a random variable with the probability density function $p(\boldsymbol{x})$. The output $Y = f(\boldsymbol{X})$ is then also a random variable and the distribution of Y is known as the uncertainty distribution. With the posterior distribution-over-functions described by equation 5, several quantities relevant to the sensitivity analysis can be inferred: the main effects and interactions, as well as the sensitivity measures including Main Effects Indices (MEI) and Total Effects Indices (TEI).

4.2.1 *Main Effects*

The function $f(\boldsymbol{x})$ can be decomposed into main effects and interactions:

$$y = f(\boldsymbol{x}) = E(Y) + \sum_{i=1}^{d} z_i(\boldsymbol{x}_i) + \sum_{i<j}^{d} z_{i,j}(\boldsymbol{x}_{i,j}) + \sum_{i<j<k}^{d} z_{i,j,k}(\boldsymbol{x}_{i,j,k}) + \ldots + z_{1,2,d}(\boldsymbol{x}) \tag{6}$$

$$z_i(x_i) = E(Y|x_i) - E(Y) \tag{7}$$

$$z_{i,j}(\boldsymbol{x}_{i,j}) = E(Y|\boldsymbol{x}_{i,j}) - z_i(x_i) - z_j(x_j) - E(Y) \tag{8}$$

Here $z_i(x_i)$ represents the main effect of $x_i, z_{i,j}(\boldsymbol{x}_{i,j})$ is the first order interaction and further terms represent higher order interactions. $E(Y)$ is the expected value of the output y considering all possible combinations of inputs. The main effect of an input is the effect (on the output) of varying that parameter over its input range, averaged over all the other inputs. Interactions describe the effect of varying two or more parameters simultaneously, additional to the main effects of both parameters. The posterior mean values for main effects and interactions can be inferred by substituting the posterior mean from equation 5 into the conditional expectation:

$$E(Y|\boldsymbol{x}_i) = \int_{\chi_{-i}} f(\boldsymbol{x}) p(\boldsymbol{x}_{-i}|\boldsymbol{x}_i) d\boldsymbol{x}_{-i} \tag{9}$$

where χ_{-i} is the sample space of $\boldsymbol{x}_{-i}$, $\boldsymbol{x}_{-i}$ is the subvector of $\boldsymbol{x}$ containing all elements except $\boldsymbol{x}_i$ and $p(\boldsymbol{x})$ represents the multivariate probability density function of the input parameters. Although this results in a series of matrix integrals, a Gaussian or uniform $p(\boldsymbol{x})$ density allows these

to be solved analytically. Expressions for interactions can also be derived with their respective definitions.

4.2.2 *Variance and Sensitivity Indices*

Variance-based sensitivity analysis quantifies the proportion of output variance for which individual input parameters are responsible. In particular, sensitivity can be measured by conditional variance:

$$V_i = var\{E(Y|X_i)\} \tag{10}$$

This is the expected value of the contribution of the input variable X_i to the output variance and is also the variance of the main effect x_i, therefore it is known as the MEI. It can be extended to measure conditional variance of interactions of inputs, for example,$V_{i,j} = var\{z_{i.j}(\boldsymbol{x}_{i,j})\}$, and so on for higher order interactions. An additional sensitivity measure, the TEI, measures the variance caused by an input x_i and any interaction of any order including x_i and describes the output variance that would remain if one were to learn the true values of all inputs except x_i:

$$V_{Ti} = var(Y) - var\{E(Y|\boldsymbol{X}_{-i})\} \tag{11}$$

The full details of the calculation of V_i and V_{Ti} can be found in [6]. All the quantities of interest presented here are calculated using the software package Gaussian Emulation Machine for Sensitivity Analysis (GEM-SA) [15].

5 Sensitivity Analysis of Flight Parameter Sensor Simulation Model

Using the discussed Bayesian sensitivity analysis technique, a sensitivity study was performed for symmetric landings using the FPSS model. The objective was to determine how sensitive the difference between 'actual' and 'simulated' loads was to the individual model parameters so that one can learn more about these parameters and reduce this difference, calculated as MSE. The input parameters include: aircraft pitch angle (*pitch*), ground speed (V_x), vertical descent velocity (V_z), longitudinal tyre-runway friction coefficient (μ), MLG shock absorber servicing state (*SA*), MLG tyre type (*tyre*), MLG tyre pressure (*tyre press*), aircraft mass (*mass*) and aircraft centre of gravity position (*CG*). In order to estimate the sensitivity measures described previously, the probability distributions for the input parameters are defined. The assumption was made that the inputs are independent, although in reality flight parameters such as pitch and ground speed are not independent and flight parameters such as roll and yaw may be coupled. The parameters can be specified as either Gaussian or uniform distributions based on how informative the available input parameter data are. In this study, the distributions have been defined as uniform distributions and the ranges of the flight parameters, normalized between zero and one, are based on typical aircraft operating limitations.

To develop the emulator, 399 combinations of input parameters were generated using a maximin Latin hypercube DOE in GEM-SA. The FPSS model was then run to provide the corresponding 'actual' and 'simulated' drag axle response loads, vertical axle response loads and bending moment at spin-up, spring-back and maximum vertical reaction. The MSE was then calculated for the loads. The sensitivity analysis was carried out in GEM-SA. The emulators were built on the first 80% of the training data and then verified using the remaining 20% of the training data. Figure 4 shows an example of the emulator accuracy for the spin-up drag axle response load MSE. Generally it was found that the emulators did a reasonable job since the model test data tended to be within the 95% confidence bands of the predictions and errors could be attributed to predicting high values of MSE since there are fewer training points for the emulator in these regions.

5.1 Main Effects Plots

The main effects plots for the analysis show MSE versus the normalised flight parameters. The lines represent mean main effects values, averaged over variations in the other parameters and can be thought of as the expected value of the output with respect to one parameter if the true

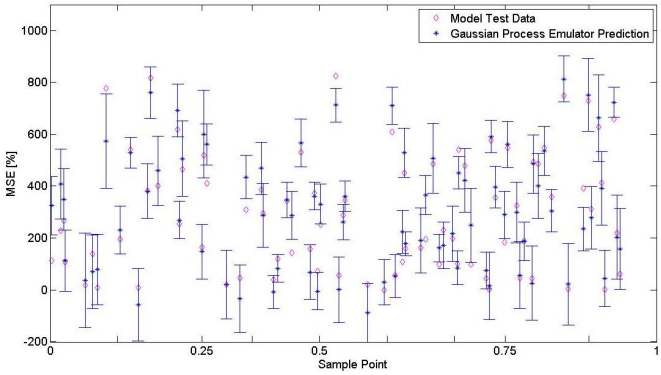

Fig. 4 Symmetric Spin Up Drag Axle Response Load Emulator Accuracy

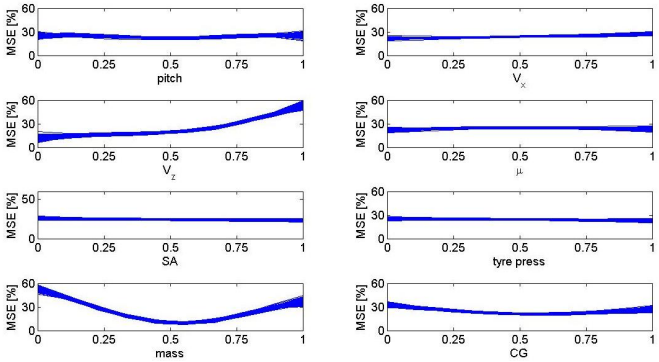

Fig. 6 Symmetric Maximum Vertical Reaction Vertical Axle Response Load Main Effects Plots

values of the other parameters are known. These plots show which of the flight parameters the MSE is significantly sensitive to and the nature of the input/output relationships. The main effects plots for drag axle response load MSE and bending moment MSE at spin-up and spring-back show the same trends. The spin-up drag axle response load main effects plots are shown in Figure 5. The maximum vertical reaction vertical axle response load main effects plots are shown in Figure 6. The main effects plot for *tyre* was not illustrated because a discrete uniform distribution was assigned to each tyre. In GEM-SA, this was described by a continuous distribution and the main effects plots are not meaningful.

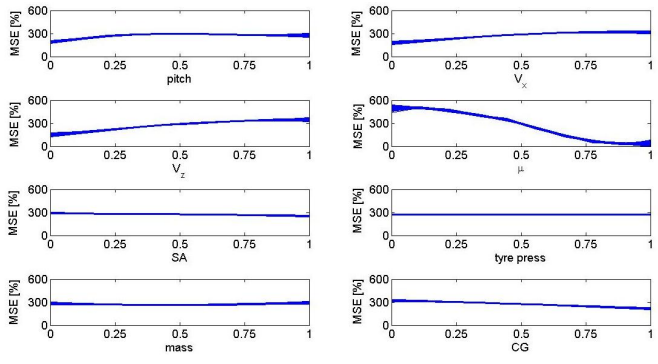

Fig. 5 Symmetric Spin Up Drag Axle Response Load Main Effects Plots

5.1.1 Aircraft Pitch Angle

The main effects plots for spin-up and spring-back show that the drag axle response load MSE and bending moment MSE linearly increases as the pitch angle increases. Due to filtering and sampling, the FDR model tends to reduce the aircraft pitch angle by less than one degree, therefore it is not expected that *pitch* would have a large contribution to the MSE. Part of the relationship between *pitch* and MSE can be attributed to the constraint in the model that limits the pitch angle to 0 degrees to ensure a two-point landing. If this constraint is removed, the relationship between *pitch* and MSE tends to be more constant. The main effects plot for the vertical axle response load MSE also shows a constant relationship with *pitch*. As will be shown in section 5.2, the contribution to the MSE from *pitch* alone is low, except in the case of bending moment at spring-back. The flight parameter *pitch* tends to only be significant in the other cases when its interactions with other flight parameters are considered.

5.1.2 Tyre-Runway Friction Coefficient

Figure 5 illustrates the relationship between MSE and μ for spin-up and spring-back drag axle response load bending moment. As the actual μ for the landing approaches the value assumed within the hard landing analysis process, the difference between the 'actual' and 'simulated' loads is reduced. This is logical considering that if the 'actual' landing has a tyre-friction coefficient that is significantly lower than that assumed in the hard landing analysis process model, this will greatly contribute to the MSE.

Figure 6 shows that there is a constant relationship between MSE and μ for vertical axle response load at maximum vertical reaction. In section 5.2.3 it is also shown that μ has little contribution to the MSE.

5.1.3 Vertical Descent Velocity

The relationship between the MSE and V_z is non-linear and tends to increase and level off at high vertical descent velocities. Figure 7 illustrates the difference between the peak aircraft vertical acceleration (N_z) in the 'actual' landing and the peak N_z from the FDR model. At higher vertical descent velocities (and hence higher vertical accelerations), the possibility increases that the peak vertical acceleration will be missed on the FDR, due to low sampling rates (8 Hz) in conjunction with greater peak amplitudes. Therefore, the 'simulated' loads will be more under predicted as vertical descent velocity increases and the difference between the 'actual' and 'simulated' loads will be greater.

As discussed in section 2, V_z is an input flight parameter, however the aircraft vertical acceleration measured by the FDR model is matched in the current hard landing analysis process model by iterating V_z. In the FDR model, the vertical acceleration is sampled and filtered and therefore any loss of data will have a significant impact on the landing gear loads modelled in the current hard landing analysis process model. Therefore, the vertical acceleration is one of the most important parameters in reducing the MSE.

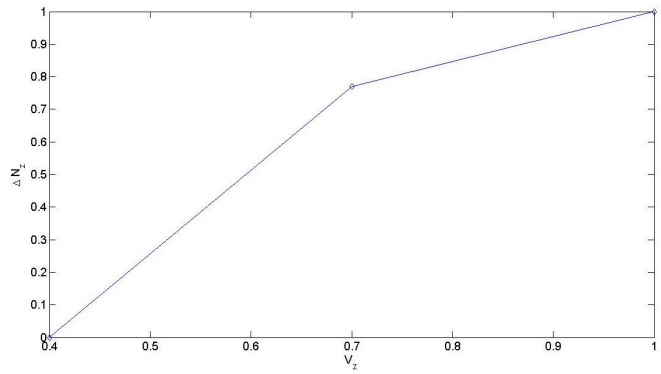

Fig. 7 Effect of Sampling on Peak Vertical Acceleration

5.1.4 Ground Speed

As V_x increases, the time required for spin-up, the maximum drag ground-to-load and the vertical ground-to tyre-load increases [16]. In the FDR model, filtering and sampling reduces the aircraft ground speed by less than 1 m/s. This is consistent with the fact that ground speed is generally assumed to be constant in landing simulations. The main effect plots for V_x shows that the MSE increases as V_x increases. This indicates that as V_x increases, the loads and moments do not increase linearly. As will be shown in section 5.2, the contribution to the MSE from V_x alone is low and V_x is only significant for spin-up and spring-back when its interactions with other flight parameters are considered.

5.1.5 Shock Absorber

In all of the main effects plots, the MLG shock absorber servicing state has a constant relationship with MSE. Therefore, the MSE is not sensitive to the shock absorber servicing state over its range and any shock absorber servicing state will give similar MSE values. When the shock absorber is overinflated, higher loads are transmitted through the landing gear structure. However, because the shock absorber is stiffer (stiffer spring curve), there is a higher aircraft vertical acceleration for the same vertical descent velocity. In the hard landing analysis process model, the peak vertical aircraft acceleration is matched by iterating V_z. Therefore, if the correctly serviced shock absorber is used in the hard landing analysis process model, a higher V_z will be required to match the vertical acceleration. Due to the fact that the vertical acceleration is being matched, the difference between the vertical and drag axle response loads and the bending moment from the landing with an overinflated shock absorber and from the landing with a correctly serviced shock absorber will be very similar.

When the shock absorber is underinflated, lower loads are transmitted through the landing gear structure and there is a lower aircraft vertical acceleration for the same vertical descent velocity. Therefore, for a correctly serviced shock

absorber, the aircraft vertical acceleration will be higher and the loads in the 'simulated' landing will be higher and therefore, more conservative.

5.1.6 *Tyre Pressure*

In all of the main effects plots, the MLG tyre pressure has a constant relationship with MSE. This indicates that the MSE is not sensitive to tyre pressure over its range and any value of the tyre pressure will give similar output values. Therefore, knowing the tyre pressure is not useful in reducing the MSE.

5.1.7 *Mass & Centre of Gravity*

The main effects plots for drag axle response load and bending moment at spin-up and spring-back show that the MSE is generally constant over the range of *mass* and the *CG*. However, the main effects plots for the maximum vertical reaction vertical axle response load MSE shows a non-linear relationship with *mass* and *CG*. As expected, as the *mass* and *CG* in the 'actual' landing moves closer to or further from the *mass* and *CG* in the 'simulated' landing, the MSE increases. This trend is more prevalent in the main effects plots for the vertical axle response load MSE than for spin-up and spring-back drag and bending moment MSE and is expected since the MEI and TEI, presented in section 5.2.3, indicate that *mass* and *CG* are very significant to the vertical axle response load.

5.2 Main Effects Indices and Total Effects Indices

The MEI plots for spin-up, spring-back and maximum vertical reaction represent the expected value of the contribution of the input flight parameter to the MSE. A high MEI means that the MSE will be reduced considerably if one were to learn the true value of that flight parameter. The TEI represent the contribution from one flight parameter if all its interactions with the other parameters are included. While an input parameter may have a low MEI, the TEI indicates if its first order and higher order interactions are significant.

5.2.1 *Spin-Up*

The MEI and TEI for the spin-up drag axle response load are given in Figure 8. The MEI illustrate that μ and V_z contribute significantly to the spin-up drag axle response load MSE. The TEI show that along with μ and V_z, V_x and *pitch* with their interactions, contribute to the spin-up drag axle response load MSE. The first order interactions account for 20.75% of the MSE. The interactions between μ-V_z (11.71%), μ-*pitch* (1.82%), μ-V_x (1.71%) and V_z-V_x (2.03%) account for approximately 17% of the MSE.

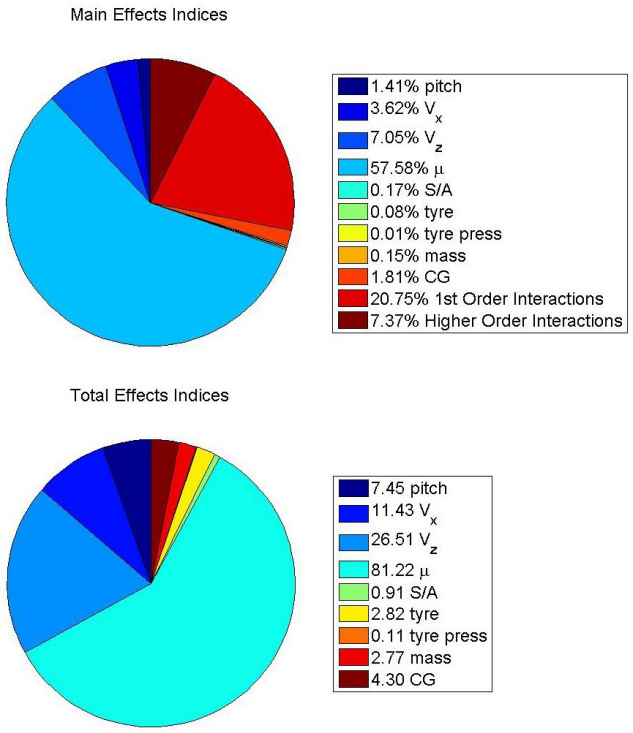

Fig. 8 Symmetric Spin-Up Drag Axle Response Load MEI and TEI

The MEI and TEI for the spin-up bending moment are given in Figure 9. The results are similar to the spin-up drag axle response load MSE. As discussed in the landing dynamics in section 2, one would expect μ, V_z and V_x would be influential in calculated spin-up and spring-back drag axle response and resulting bending moment. Any change in these parameters due to the FDR or assumptions that are made in the hard landing analysis process model would have an effect on the MSE. Therefore, the spin-up drag axle

response load MSE and bending moment MSE may be reduced by learning the true value of μ and V_z.

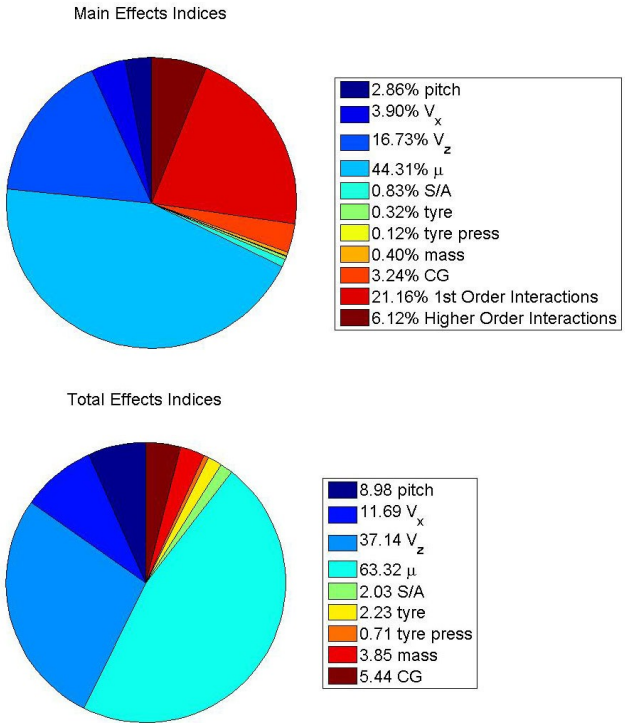

Fig. 9 Symmetric Spin-Up Bending Moment at Lower Bearing MEI and TEI

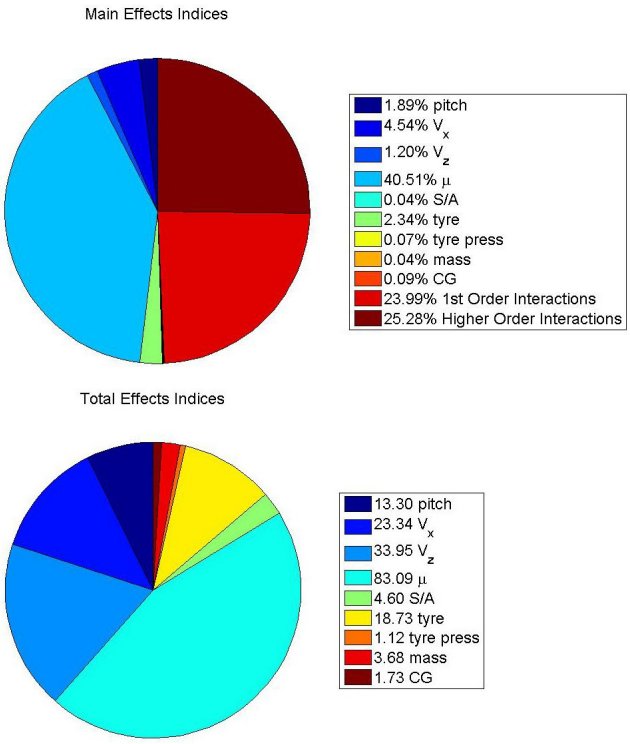

Fig. 10 Symmetric Spring Back Drag Axle Response Load MEI and TEI

5.2.2 *Spring-Back*

The MEI and TEI for the spring-back drag axle response load are given in Figure 10. The MEI and TEI again show similar results to the spin-up drag axle response load, in that μ, V_z, V_x and pitch contribute significantly. However, the TEI also shows that tyre and its interactions have an effect on the the spring-back drag axle response load MSE. The following first order interactions account for approximately 19% of the MSE: μ-V_z (9.56%), μ-V_x (3.04%), μ-*pitch* (2.96%), μ-*tyre* (2.28%) and V_z-*tyre* (1.31%). Therefore, *tyre*, due to its interaction with μ and V_z, is an important parameter in the spring-back drag axle response load MSE.

The MEI and TEI for the spring-back bending moment MSE are given in Figure 11. Again, μ, V_z, V_x, *pitch* and *tyre* contribute significantly. The following interactions account for approximately 24% of the MSE: μ-V_z (5.95%), μ-*pitch* (13.88%), μ-*mass* (2.36%) and V_x-*pitch* (2.41%). Therefore, *mass* is also a significant parameter for spring-back bending moment MSE. The spring-back drag axle response load MSE and bending moment MSE may be reduced by learning the true value of μ, V_z, *tyre* and *mass*.

5.2.3 *Maximum Vertical Reaction*

The vertical axle response load at maximum vertical reaction is of interest when calculating the landing gear loads. The MEI and TEI for the vertical axle response load MSE are given in Figure 12. The MEI illustrate that mass and V_z contribute significantly to the vertical axle response load MSE. The TEI show that along with mass and V_z, CG, pitch and tyre with their interactions, contribute to the vertical axle response load MSE. The first order interactions account for 49% of the MSE. The interactions between *mass*-CG (14.68%), *mass-pitch* (14.19%), V_z-*CG* (4.17%), V_z-*pitch* (2.33%), *mass-tyre* (2.11%) account for approximately 37% of the MSE. There-

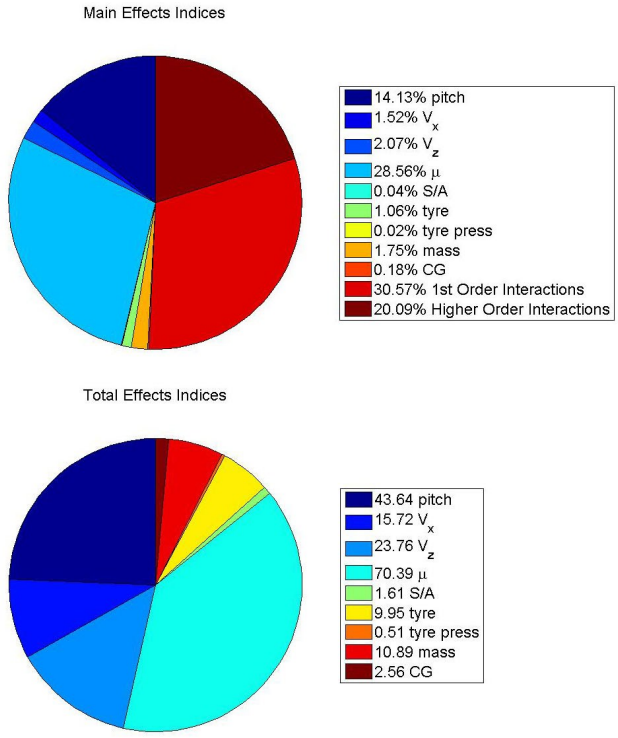

Fig. 11 Symmetric Spring Back Moment at Lower Bearing MEI and TEI

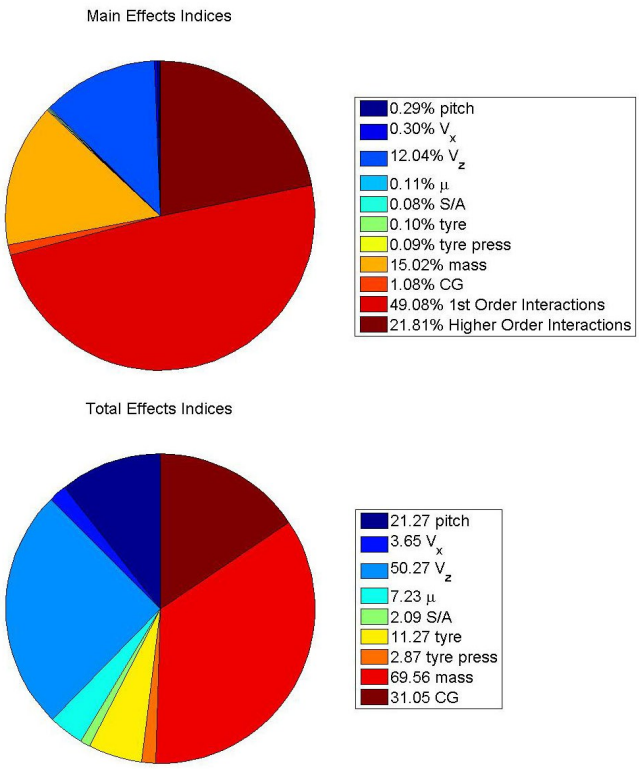

Fig. 12 Symmetric Maximum Vertical Reaction Vertical Axle Response Load MEI and TEI

fore, the vertical axle response load MSE may be reduced by learning the true value of *mass*, V_z, *CG* and *tyre*.

6 Conclusion

A Bayesian sensitivity analysis was performed to determine the parameters of interest in order to reduce the conservatism calculated in the FPSS model. For symmetric two-point landings, it was shown that tyre-runway friction coefficient and aircraft vertical descent velocity contributed the most to the spin-up and spring back drag axle response load MSE and bending moment MSE. It was also found that aircraft vertical descent velocity, mass, centre of gravity position and MLG tyre type had significant influences on the maximum vertical reaction vertical axle response load MSE. While V_x and *pitch* did not change considerably from the 'actual' to the 'simulated' landing, the interactions with μ and V_z contributed to the MSE in all cases. Therefore, the MSE can be reduced by learning the true value of the following flight parameters: μ, V_z, *mass*, *CG* and *tyre type*. Due to the current hard landing analysis process modelling technique, vertical acceleration is as significant as V_z in reducing MSE. It was also shown that over the range in this sensitivity study, the shock absorber servicing state and MLG tyre pressure do not contribute significantly to the MSE and learning the true value of these flight parameters would not reduce the MSE.

This technique will be extended to asymmetric landings and will consider other flight parameters such as lateral velocity, aircraft roll and aircraft yaw. The effect of signal processing on the aircraft flight parameters will also be investigated. The results of the sensitivity analysis will then used in the conceptual design of sensor and data acquisition system architectures that improve the accuracy of the calculated loads.

References

[1] "Certification Specifications for Large Aeroplanes, CS25," 2008.

[2] "Airworthiness Standards: Transport Category Airplanes, FAR 25," 2008.

[3] Sartor, P., Bond, D., Staszewski, W., and Schmidt, R. K., "Assessment of the Value of an Overload Indication System through Analysis of Aviation Industry Occurrence Data," *AIAA Journal of Aircraft*, Vol. 46, No. 5, 2009, pp. 1692–1705.

[4] Sartor, P., Schmidt, R. K., Menezes, R., Bond, D., and Staszewski, W., "Validation and Verification of a Hard Landing Indication System for Aircraft Landing Gear," *Proceedings of 7th International Workshop on Structural Health Monitoring*, Stanford, U.S.A., 2009, pp. 190–200.

[5] Saltelli, A., Chan, K., and Scott, E. M., *Sensitivity Analysis*, Wiley, 2000.

[6] Oakley, J. E. and O'Hagen, A., "Probabilistic Sensitivity Analysis of Complex Models: A Bayesian Approach," *Journal of the Royal Statistical Society Series B*, Vol. 66, No. 3, 2004, pp. 751–769.

[7] Worden, K. and Becker, W., "On the Identification of Hysteretic Systems, Part II: Bayesian Sensitivity Analysis." *Proceedings of the XXVIII International Modal Analysis Conference & Exposition on Structural Dynamics*, Jacksonville, Florida, U.S.A., 2010.

[8] Wright, J. R. and Cooper, J. E., *Introduction to Aircraft Aeroelasticity and Loads*, Wiley, 2007.

[9] Currey, N. S., *Aircraft Landing Gear Design: Principles and Practices*, American Institute of Aeronautics and Astronautics, Washington, D.C., 1988.

[10] Milwitzky, B., Lindquist, D., and Potter, D., "An Experimental Study of Applied Ground Loads in Landing," Tech. Rep. 1248, NACA, 1955.

[11] Lomax, T. L., *Structural Loads Analysis for Commercial Transport Aircraft: Theory and Practice*, AIAA Education Series, 1996.

[12] Kennedy, M. C., Anderson, C. W., Conti, S., and O'Hagen, A., "Case Studies in Gaussian Process Modelling of Computer Codes," *Reliability Engineering and System Safety*, Vol. 91, No.10-11, 2006, pp. 1301–1309.

[13] Kennedy, M. C. and O'Hagen, A., "Bayesian Calibration of Computer Models," *Journal of the Royal Statistical Society: Series B (Statistical Methodology)*, Vol. 63, No. 3, 2001, pp. 425–464.

[14] Sacks, J., Welch, W. J., Mitchell, T. J., and Wynn, H. P., "Design and Analysis of Computer Experiments," *Statistical Science*, Vol. 4, No. 4, 1989, pp. 409–435.

[15] Kennedy, M. C., "GEM-SA Homepage," http://ctcd.group.shef.ac.uk/gem.html.

[16] Milwitzky, B., Lindquist, D., and Potter, D., "An Experimental Study of Wheel Spin-Up Drag Loads," Tech. Rep. 3246, NACA, 1954.

7 Acknowledgements

The authors would like to thank the following colleagues for their invaluable assistance in the model development and sensitivity study analysis: Laura Collett, Julia Payne, Sidney Smith and Andrew Thomas.

8 Contact Author Email Address

p.sartor@sheffield.ac.uk

9 Copyright Statement